

Fracture of disordered three-dimensional spring networks: A computer simulation methodology

J. W. Chung, A. Roos, and J. Th. M. De Hosson

Department of Applied Physics, Materials Science Centre, University of Groningen, Nijenborgh 4, 9747 AG Groningen, The Netherlands.

E. van der Giessen

Laboratory for Engineering Mechanics, Delft University of Technology, Delft, The Netherlands

(Received 6 May 1996; revised manuscript received 9 July 1996)

In this paper a computational technique is proposed to describe brittle fracture of highly porous random media. Geometrical heterogeneity in the “open cell foam” structure of the porous medium on a mesoscopic length scale (~ 100 nm) is mapped directly onto a three-dimensional (3D) elastic network by using molecular dynamics techniques to generate starting configurations. The aspects in our description are that the elastic properties of an *irregular 3D-network* are described using not only a potential with a two-body term (change in bond length, or linear elastic tension) and a three-body term (change in bond angle, or bending), but also a four-body term (torsion). The equations for minimum energy are written and solved in matrix form. If the changes in bond lengths, bond- or torsion angles exceed pre-set threshold values, then the corresponding bonds are irreversibly removed from the network. Brittleness is mimicked by choosing small ($\sim 1\%$) threshold values. The applied stress is increased until the network falls apart into two or more pieces. [S0163-1829(96)07146-9]

I. INTRODUCTION

This paper concentrates on a methodology that is aimed at finding a relation between the mechanical strength of porous media and its microstructural features. The microstructure of a typical highly porous ceramic material is depicted in Fig. 1. The geometrical inhomogeneity of the microstructure makes the fracturing process particularly complicated because it is very sensitive to local crack formation. These local cracks can be the starting point of global failure. The modelling takes place at the length scale of the individual pores (typically ~ 100 nm, but this can be controlled to a certain extent by adjusting manufacturing parameters). The porous material is modelled as a three-dimensional, geometrically inhomogeneous network of spheres or nodes, connected by springs or beams.

Elastic networks of springs or beams are frequently used to model the relation between mechanical properties of materials and their microstructure. Simulations have been carried out both in two^{1,2,3,5} and three^{1,4,5,6,7} dimensions, mainly on regular spring networks. In these simulations, a network is loaded by an external force or displacement, after which some potential function of the nodal displacements is minimized. Mechanical properties can be studied from the resulting equilibrium configuration.

The general field of application of this work lies in the area of catalyst carriers, where highly porous ceramic materials (60–70 vol. %) are commonly used. Due to their large internal surface (up to 250 m²/g), they are well suited as catalyst carriers for chemical processes (Fig. 1).^{1,8} The catalyst carriers exhibit brittle fracture behavior and when used in a reactor, they may fail due to their own weight. Crumbled catalyst carriers can block the diffusion paths of reactants through the material. Furthermore, the flow of reactants can move the debris out of the reactor, thereby reducing the reactive area. For that reason, the focal point of the methodology is to obtain a physical description of the ultimate

strength in conjunction with its size dependence. Experimentally, this is accessible through the side crushing strength (SCS), also known as the Brazilian test^{1,8} which is believed to measure indirectly the tensile strength. In this paper, the emphasis is on the methodology as such, whereas in a future paper the size dependence will be reported.

II. COMPUTATIONAL PROCEDURE

The computational procedure consists of two independent steps. The first step is the generation of a network in which a disordered configuration of spheres is obtained and connections are made. The second step consists of a sequence of applying a force and calculating the corresponding displacements and subsequently imposing fracture criteria. This sequence is repeated until the network falls apart into two (or more) pieces.

Initially, a number of spheres N is arranged on a simple cubic lattice. The spheres are given a Maxwell-Boltzmann velocity distribution at a certain temperature T . A molecular dynamics (MD) run is carried out⁹ using a Lennard-Jones potential to obtain a disordered configuration.

When the system is equilibrated, spheres that are within a predefined *cut-off radius* r_c [m] from each other are connected, using the centers of the spheres as connection points or nodes. This is the initial stress-free model for the geometry in Fig. 2.

The top surface is defined as the set of spheres lying within some pre-set vertical distance from the sphere with the largest z coordinate. The bottom surface is defined analogously. The external force is applied at the top and bottom surfaces of the network. The total force on the top surface is equal in magnitude but opposite in direction as the total force on the bottom surface. The other surfaces are not constrained, so the network is free to expand in the horizontal directions, conform the configuration in the SCS.

A brittle material can only withstand small deformations.

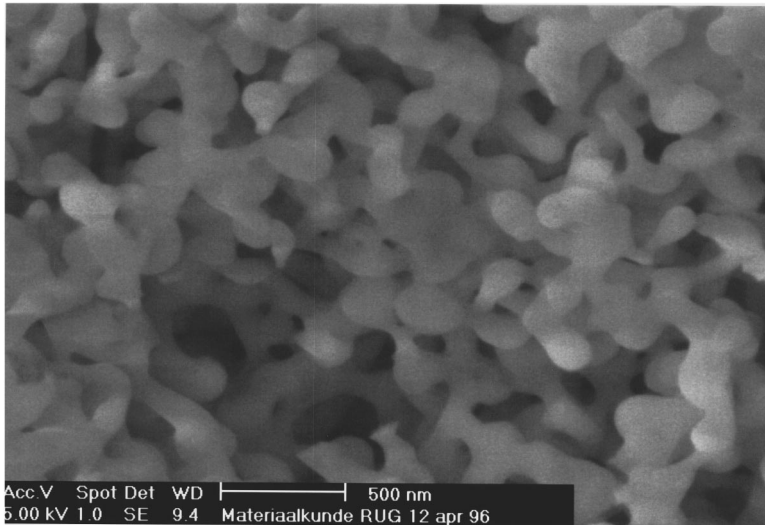


FIG. 1. Typical microstructure of a SiO_2 extrudate.

This is captured in the model by imposing a fracture criterion on the bonds. If a bond is stretched or compressed beyond a pre-set value, or if a bond or torsion angle change exceeds a threshold, the bond is irreversibly removed from the network. The local stress has to be redistributed through the remaining bonds, leading to a new equilibrium configuration. Other bonds or angles that now fulfill the fracture criteria are removed from the network. Brittle fracture of the bonds is modelled by allowing only small length and angle changes. This also ensures that the elastic behavior remains linear in terms of the nodal displacements.

By increasing the external stress, this process eventually leads to global failure. The step size at which the force increases should be large enough to limit the time of the total simulation. On the other hand, if the step is too large, too many bonds will break in one step, which makes it difficult to monitor crack formation and propagation.

The system is in equilibrium for given internal and external stresses when a minimum in the total energy is reached. The total elastic energy consists of a two-body *central force* (CF), a three-body *bond-bending* (BB) and a four-body *torsion* (T) contribution:

$$U_{EL} = U_{CF} + U_{BB} + U_T. \quad (1)$$

In the new equilibrium configuration, the fracture criteria can be applied. In the present model, three fracture criteria are adopted: one for elongation (compression), one for bond angle change, and one for torsion angle change. The elongation and compression criterion is fulfilled when the strain of a bond is larger than a pre-set value Δ_{CF} . In that case, the bond is removed from the network. Similarly, if the change in bond angle exceeds a threshold Δ_{BB} , the bond with the largest change in bond angle from its unloaded equilibrium

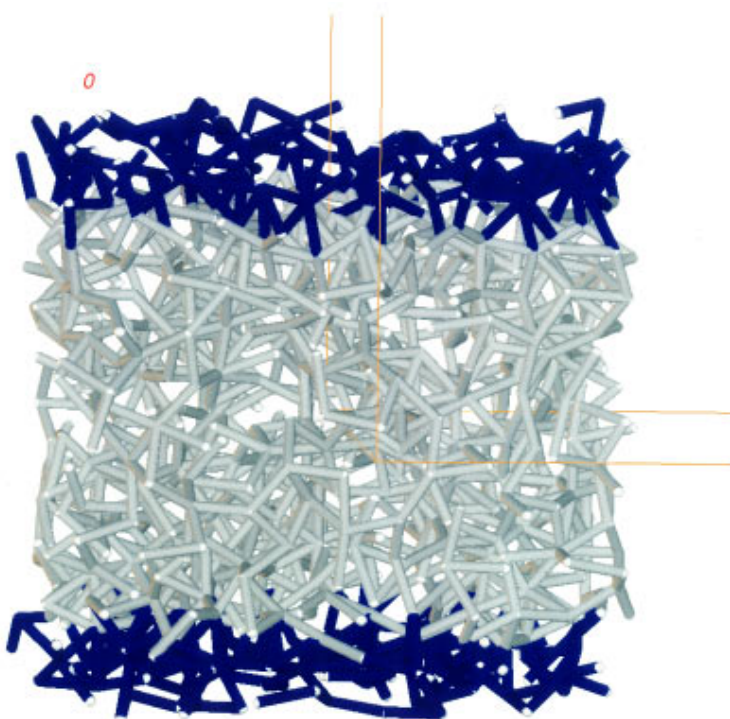


FIG. 2. A geometrically disordered, three-dimensional network (1000 nodes). Blue bonds are connected to nodes in the top or bottom layers.

position is removed. Finally, a threshold Δ_T is imposed on the torsion angle per unit length, beyond which the bond is removed. The values of Δ_{CF} , Δ_{BB} , and Δ_T do not necessarily have to be the same for all bonds, but can be distributed over the network according to some probability distribution,⁵ thus mimicking possible inhomogeneities in the yield strength of the material on the pore size scale. Brittleness is mimicked by choosing small ($\sim 1\%$) threshold values. When some bonds have been removed, the stress has to redistribute itself along the remaining bonds. The external stress may also change. Under these conditions, the equilibrium configuration changes, so the procedure described above has to be iterated. After a number of increments, so many bonds have broken that there is no longer a percolating cluster of bonds: the system has fallen apart into two (or more) pieces.

In this work, linear elasticity and small displacements of the spheres are assumed, so the displacements enter quadratically in the potential energy. This is ensured by the aforementioned choice of brittle fracture criteria. In the following the description of the potential is given in a concise way (convention: \mathbf{A} is a vector in R^3 , with components A^q ($q \in \{x, y, z\}$)[m] and length $|\mathbf{A}| \equiv \sqrt{(A^x)^2 + (A^y)^2 + (A^z)^2}$ [m]. Also, $\hat{\mathbf{A}} \equiv \mathbf{A}/|\mathbf{A}|$).

The central force (CF) contribution consists of a Hookean spring potential:

$$\begin{aligned} U_{CF}(n+1) &= \frac{1}{2} \sum_{\langle ij \rangle} k_{ij}^{CF} [|\mathbf{R}_{ij}(n+1)| - |\mathbf{R}_{ij}(0)|]^2 \\ &\approx \frac{1}{2} \sum_{\langle ij \rangle} k_{ij}^{CF} [\Delta \mathbf{u}_{ij}(n+1) \cdot \hat{\mathbf{R}}_{ij}(n) \\ &\quad + (|\mathbf{R}_{ij}(n)| - |\mathbf{R}_{ij}(0)|)]^2, \end{aligned} \quad (2)$$

where the summation is over all $\langle ij \rangle$ pairs of connected neighbors. The bond vector $\mathbf{R}_{ij}(n)[m]$ from node i to node j (\equiv bond ij) at increment n is defined as $\mathbf{r}_j(n) - \mathbf{r}_i(n)$, where $\mathbf{r}_i(n)[m]$ is the position vector of node i at increment n . Furthermore, the displacement increment $\Delta \mathbf{u}_{ij}(n)[m]$ at increment n is given by $\Delta \mathbf{u}_i(n) - \Delta \mathbf{u}_j(n)$, with $\Delta \mathbf{u}_i(n) \equiv \mathbf{u}_i(n+1) - \mathbf{u}_i(n)[m]$ the displacement increment of node i and $\mathbf{u}_i(n) \equiv \mathbf{r}_i(n) - \mathbf{r}_i(0)[m]$ the displacement of node i at increment n . The force constant $k_{ij}^{CF}[N/m]$ of bond ij (the *CF-constant*) is written as

$$k_{ij}^{CF} = \frac{A_{ij} E_{ij}}{|\mathbf{R}_{ij}(0)|}, \quad (3)$$

with $A_{ij}[m^2]$ the cross-sectional area of bond ij (all cross sections are assumed to be circular) and $E_{ij}[N/m^2 \equiv Pa]$ its Young's modulus.

For the bond-bending potential term, consider triplets of spheres i , j , and k , with j and k at a distance less than r_c of the central sphere i (Fig. 3). The relevant term is $\theta_{ijk}(n)$, the total *change* of bond angle between bonds ij and ik at increment n , relative to the initial bond angle [i.e., $\theta_{ijk}(0) \equiv 0$]. The bond angle increment $\Delta \theta_{ijk}(n+1) \equiv \theta_{ijk}(n+1) - \theta_{ijk}(n)$ can be split into $\Delta \theta_{ijk}^{ij}(n+1)$, the bond angle change due to $\Delta \mathbf{u}_{ij}(n+1)$ only, keeping \mathbf{R}_{ik} fixed, and $\Delta \theta_{ijk}^{ik}(n+1)$, defined analogously:

$$\Delta \theta_{ijk}(n+1) = \Delta \theta_{ijk}^{ij}(n+1) + \Delta \theta_{ijk}^{ik}(n+1). \quad (4)$$

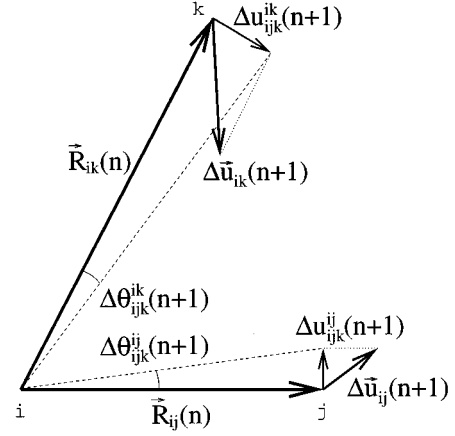


FIG. 3. Three-body potential.

The bond-bending potential is given by

$$\begin{aligned} U_{BB}(n+1) &= \frac{1}{2} \sum_{\langle ijk \rangle} k_{ijk}^{BB} \theta_{ijk}^2(n+1) \\ &= \frac{1}{2} \sum_{\langle ijk \rangle} k_{ijk}^{BB} [\Delta \theta_{ijk}^{ij}(n+1) \\ &\quad + \Delta \theta_{ijk}^{ik}(n+1) + \theta_{ijk}(n)]^2, \end{aligned} \quad (5)$$

where the summation is over all $\langle ijk \rangle$ triplets as in Fig. 3. $k_{ijk}^{BB}[Nm]$ is the three-body force constant (the *BB-constant*) between nodes i , j , and k . The (small) change in bond angle $\Delta \theta_{ijk}(n+1)$ is related to the component of the displacements $\Delta \mathbf{u}_{ij}(n+1)$ and $\Delta \mathbf{u}_{ik}(n+1)$ in the plane defined by spheres i, j, k , in the direction orthogonal to $\mathbf{R}_{ij}(n)$ and $\mathbf{R}_{ik}(n)$, respectively. The components of the displacements $\Delta \mathbf{u}_{ij}^{ij}(n+1)$ and $\Delta \mathbf{u}_{ik}^{ik}(n+1)$ in the i, j, k plane in these directions become (a slightly different approach can be found in Wang⁶):

$$\Delta \mathbf{u}_{ij}(n+1) \cdot \left(\frac{[\mathbf{R}_{ik}(n) \times \mathbf{R}_{ij}(n)] \times \mathbf{R}_{ij}(n)}{|[\mathbf{R}_{ik}(n) \times \mathbf{R}_{ij}(n)] \times \mathbf{R}_{ij}(n)|} \right) \equiv \Delta \mathbf{u}_{ij}^{ij}(n+1) \quad (6)$$

and

$$\Delta \mathbf{u}_{ik}(n+1) \cdot \left(\frac{[\mathbf{R}_{ij}(n) \times \mathbf{R}_{ik}(n)] \times \mathbf{R}_{ik}(n)}{|[\mathbf{R}_{ij}(n) \times \mathbf{R}_{ik}(n)] \times \mathbf{R}_{ik}(n)|} \right) \equiv \Delta \mathbf{u}_{ik}^{ik}(n+1). \quad (7)$$

For small changes in bond angle, the following approximation can be made:

$$\begin{aligned} \Delta \theta_{ijk}(n+1) &\approx \tan[\Delta \theta_{ijk}^{ij}(n+1)] + \tan[\Delta \theta_{ijk}^{ik}(n+1)] \\ &= \frac{\Delta \mathbf{u}_{ij}^{ij}(n+1)}{|\mathbf{R}_{ij}(n)|} + \frac{\Delta \mathbf{u}_{ik}^{ik}(n+1)}{|\mathbf{R}_{ik}(n)|}, \end{aligned} \quad (8)$$

so that $\Delta \theta_{ijk}^{ij}(n+1)$ and $\Delta \theta_{ijk}^{ik}(n+1)$ can be written as

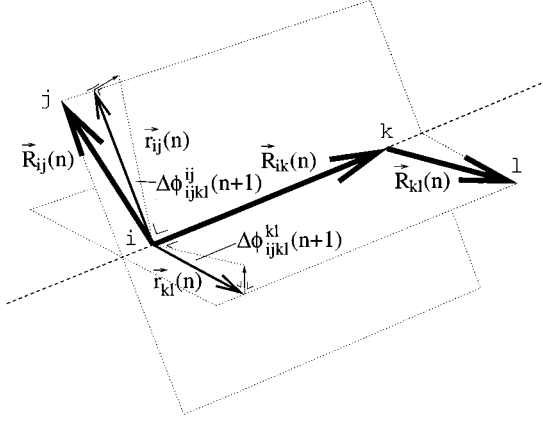


FIG. 4. Four-body potential. $\Delta\phi_{ijkl}^{ij}(n+1)$ and $\Delta\phi_{ijkl}^{kl}(n+1)$ are defined in an analogous fashion as $\Delta\theta_{ijk}^{ij}(n+1)$ and $\Delta\theta_{ijk}^{ik}(n+1)$ in the three-body potential, with $\Delta\phi_{ijkl}(n+1) = \Delta\phi_{ijkl}^{ij}(n+1) + \Delta\phi_{ijkl}^{kl}(n+1)$.

$$\begin{aligned} \Delta\theta_{ijk}^{ij}(n+1) &= \Delta\mathbf{u}_{ij}(n+1) \\ &\times \left(\frac{[\hat{\mathbf{R}}_{ik}(n) \cdot \hat{\mathbf{R}}_{ij}(n)]\hat{\mathbf{R}}_{ij}(n) - \hat{\mathbf{R}}_{ik}(n)}{|\mathbf{R}_{ij}(n)|\sqrt{1 - [\hat{\mathbf{R}}_{ij}(n) \cdot \hat{\mathbf{R}}_{ik}(n)]^2}} \right) \\ &\equiv \Delta\mathbf{u}_{ij}(n+1) \cdot \mathbf{B}_j, \end{aligned} \quad (9)$$

$$\begin{aligned} \Delta\theta_{ijk}^{ik}(n+1) &= \Delta\mathbf{u}_{ik}(n+1) \\ &\times \left(\frac{[\hat{\mathbf{R}}_{ij}(n) \cdot \hat{\mathbf{R}}_{ik}(n)]\hat{\mathbf{R}}_{ik}(n) - \hat{\mathbf{R}}_{ij}(n)}{|\mathbf{R}_{ik}(n)|\sqrt{1 - [\hat{\mathbf{R}}_{ij}(n) \cdot \hat{\mathbf{R}}_{ik}(n)]^2}} \right) \\ &\equiv \Delta\mathbf{u}_{ik}(n+1) \cdot \mathbf{B}_k. \end{aligned} \quad (10)$$

Furthermore, $\theta_{ijk}(n)$ is given by

$$\theta_{ijk}(n) = \arccos[\hat{\mathbf{R}}_{ij}(n) \cdot \hat{\mathbf{R}}_{ik}(n)] - \arccos[\hat{\mathbf{R}}_{ij}(0) \cdot \hat{\mathbf{R}}_{ik}(0)]. \quad (11)$$

The restoring force is modelled as originating from sphere i , which acts as a hinge. In order to find a reasonable expression for the BB force constant for this hinge, an analogy is drawn with the theory of bending beams. From elasticity theory,¹⁰ the force constant for a bending beam ij is given by (with $I_{ij}[m^4]$ the second moment of area of bond ij):

$$k_{ijk}^{ij, BB} = \frac{3E_{ij}I_{ij}}{|\mathbf{R}_{ij}(n)|} \quad (12)$$

and analogously for bond ik . Equating the torques acting on the ijk system in equilibrium yields an expression for the force constant:

$$k_{ijk}^{BB} = \left(\frac{|\mathbf{R}_{ij}(n)|}{3E_{ij}I_{ij}} + \frac{|\mathbf{R}_{ik}(n)|}{3E_{ik}I_{ik}} \right)^{-1}. \quad (13)$$

The reason for using an overall constant, instead of one for each beam, is that the latter case would lead to *two two-body* potential terms, one for each beam. As a result, this cannot describe any rotations of the total ijk system, and $\Delta\theta_{ijk}^{ij}$ and $\Delta\theta_{ijk}^{ik}$ are considered independently.

The change in torsion angle $\phi_{ijkl}(n)$ is defined as the total *change* of torsion angle of bond ik at increment n , relative to the initial torsion angle [i.e., $\phi_{ijkl}(0) \equiv 0$]. It is the angle between (the projection of bond ij on a plane with normal in the direction of bond ik) and (the projection of bond kl on the same plane). This angle enters quadratically into the torsion (T) potential (Fig. 4):

$$\begin{aligned} U_T(n+1) &= \frac{1}{2} \sum_{\langle ijkl \rangle} k_{ijkl}^T \phi_{ijkl}^2(n+1) \\ &= \frac{1}{2} \sum_{\langle ijkl \rangle} k_{ijkl}^T [\Delta\phi_{ijkl}(n+1) + \phi_{ijkl}(n)]^2, \end{aligned} \quad (14)$$

where $\Delta\phi_{ijkl}(n+1) \equiv \phi_{ijkl}(n+1) - \phi_{ijkl}(n)$ is the torsion angle increment. From elasticity theory,¹⁰ the force constant (T -constant) between nodes i , j , k , and l is given by (where ν is Poisson's ratio):

$$k_{ijkl}^T = \frac{E_{ik}I_{ik}}{(1+\nu)|\mathbf{R}_{ik}(n)|}. \quad (15)$$

The summation in (14) is over all quadruplets $\langle ijkl \rangle$ of spheres with (spheres j and k within r_c of sphere i) and (sphere l within r_c of sphere k). The problem can effectively be reduced to the three-body problem by projecting bonds ij and kl onto the plane normal to bond ik . Defining

$$\begin{aligned} \mathbf{r}_{kl}(n) &\equiv \mathbf{R}_{kl}(n) - [\mathbf{R}_{kl}(n) \cdot \hat{\mathbf{R}}_{ik}(n)]\hat{\mathbf{R}}_{ik}(n), \\ \mathbf{r}_{ij}(n) &\equiv \mathbf{R}_{ij}(n) - [\mathbf{R}_{ij}(n) \cdot \hat{\mathbf{R}}_{ik}(n)]\hat{\mathbf{R}}_{ik}(n) \end{aligned} \quad (16)$$

and proceeding with $\mathbf{r}_{ij}(n)$ and $\mathbf{r}_{kl}(n)$ as in the BB case, $\Delta\phi_{ijkl}(n+1)$ can be written as

$$\begin{aligned} \Delta\phi_{ijkl}(n+1) &= \Delta\mathbf{u}_{ij}(n+1) \\ &\times \left(\frac{\hat{\mathbf{R}}_{ij}(n) \times \hat{\mathbf{R}}_{ik}(n)}{|\mathbf{R}_{ij}(n)|\{1 - [\hat{\mathbf{R}}_{ij}(n) \cdot \hat{\mathbf{R}}_{ik}(n)]^2\}} \right) \\ &+ \Delta\mathbf{u}_{kl}(n+1) \\ &\times \left(\frac{\hat{\mathbf{R}}_{kl}(n) \times \hat{\mathbf{R}}_{ik}(n)}{|\mathbf{R}_{kl}(n)|\{1 - [\hat{\mathbf{R}}_{kl}(n) \cdot \hat{\mathbf{R}}_{ik}(n)]^2\}} \right) \\ &\equiv \Delta\mathbf{u}_{ij}(n+1) \cdot \mathbf{T}_j + \Delta\mathbf{u}_{kl}(n+1) \cdot \mathbf{T}_l. \end{aligned} \quad (17)$$

The angle change $\phi_{ijkl}(n)$ is given by

$$\phi_{ijkl}(n) = \arccos[\hat{\mathbf{r}}_{kl}(n) \cdot \hat{\mathbf{r}}_{ij}(n)] - \arccos[\hat{\mathbf{r}}_{kl}(0) \cdot \hat{\mathbf{r}}_{ij}(0)]. \quad (18)$$

In the expression for U_{CF} [Eq. (2)] the $[|\mathbf{R}_{ij}(n)| - |\mathbf{R}_{ij}(0)|]$ term is a constant for increment $(n+1)$. It represents the central force between spheres i and j already present at the beginning of increment $(n+1)$. The same holds for the $\theta_{ijk}(n)$ term in the three-body case and the $\phi_{ijkl}(n)$ term in the four-body case. In other words, the system is not relaxed

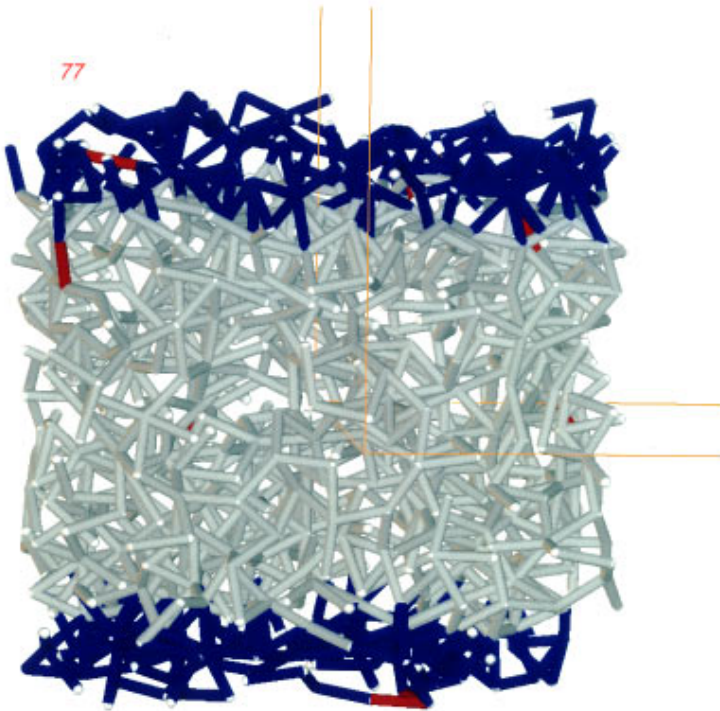


FIG. 5. Intermediate stage in the fracturing process. Red bonds fulfill a fracture criterion.

or stressfree before the next increment. The force $\mathbf{F}_\alpha^q[N]$ on sphere α in the q direction consists therefore of two contributions:

$$\begin{aligned} F_\alpha^q(n+1) &= [F_\alpha^q(n+1) - F_\alpha^q(n)] + F_\alpha^q(n) \\ &\equiv \Delta F_\alpha^q(n+1) + F_\alpha^q(n). \end{aligned} \quad (19)$$

Applying this to *one* $\langle ij \rangle$ pair in U_{CF} gives the *reaction* force increment on node i :

$$\begin{aligned} \Delta F_i^{CF,q}(n+1) &= - \left(- \frac{\partial U^{CF}(n+1)}{\partial q_i} (n+1) \right) \\ &= -k_{ij}^{CF} [\Delta \mathbf{u}_{ij}(n+1) \cdot \hat{\mathbf{R}}_{ij}(n)] \hat{\mathbf{R}}_{ij}^q(n). \end{aligned} \quad (20)$$

The contributions of all $\langle ij \rangle$ pairs are added into a *global stiffness matrix* relating the displacements in the three coordinate directions of all spheres to all force increments in these directions. The same procedure is applied to the *BB*

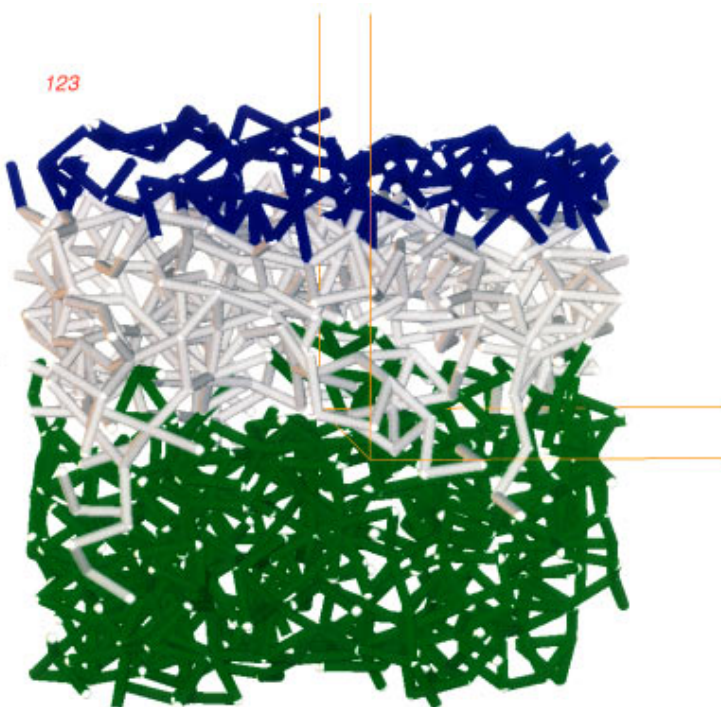


FIG. 6. Final stage of global failure. The network has fallen apart into two separate parts, one of which is colored green.

and T contributions. When all entries are added into the global matrix, a system of (three times the number of spheres) linear equations is formed, or

$$\Delta \mathbf{F}(n+1) = [K] \Delta \mathbf{u}(n+1), \quad (21)$$

where $\Delta \mathbf{F}(n+1)$ is a $3N$ -dimensional vector of the applied force increments at iteration step n , $[K]$ the $3N \times 3N$ stiffness matrix and $\Delta \mathbf{u}(n+1)$ $3N$ -dimensional vector of the displacement increments at iteration n . The external force is applied through the force vector. The resulting displacement increments are formally found from

$$\Delta \mathbf{u}(n+1) = [K]^{-1} \Delta \mathbf{F}(n+1), \quad (22)$$

but are actually obtained by solving the system of equations using a preconditioned conjugate gradient algorithm¹¹ which exploits the fact that $[K]$ is a sparse matrix. Note that the $\mathbf{F}(n)$ terms do not explicitly enter this equation. The new positions at the end of increment $n+1$ are updated according to $\mathbf{r}_i(n+1) = \mathbf{r}_i(n) + \Delta \mathbf{u}_i(n+1)$. In Fig. 5 an intermediate result is displayed and in Fig. 6 the final configuration after complete failure is presented.

III. DISCUSSION AND CONCLUSIONS

The geometrical disorder of highly porous brittle materials can be modelled using a three-dimensional disordered spring network. Some authors¹ use a Hookean spring, or *central force (CF)*, potential. This is a two-body potential, which takes into account that the force exerted by a spring is linearly proportional to the displacement in the *axial* direction of the bond. Others^{2,4,5,7} include a three-body, or *bond-bending (BB)* term to account for the change in bond angle between neighboring bonds. The restoring force is proportional to the change in the bond angle. When bending of collinear bonds is not allowed, then the model is called the Kirkwood-Keating (KK) model. The reason for this is that for $\mathbf{R}_{ij}(n)$ parallel to $\mathbf{R}_{ik}(n)$, there is no unique plane defined by $\mathbf{R}_{ij}(n)$ and $\mathbf{R}_{ik}(n)$. The components $\Delta u_{ijk}^{ij}(n+1)$ and $\Delta u_{ijk}^{ik}(n+1)$ are only constrained by being normal to $\mathbf{R}_{ij}(n)$ and $\mathbf{R}_{ik}(n)$, respectively.⁶

To our knowledge, only one author has so far suggested that for 3D models a torsion term (a four-body potential) should be included.⁶ At present, actual application in an elastic spring network has not been found in the literature. In this work, however, two-, three- and four-body interactions are included. In the four-body potential, a similar problem as in the three-body case arises for (almost) parallel bonds. When bond ij (or kl) is almost parallel to bond ik , $|\mathbf{r}_{ij}|$ (or $|\mathbf{r}_{kl}|$) can be small enough to invalidate the approximation $\phi_{ijkl}^{ijk} \approx \tan \phi_{ijkl}^{ijk}$. This can be circumvented by the following line of reasoning for the ij case: if $|\mathbf{r}_{ij}|$ is very small, the force needed to change the torsion angle significantly is very large. Also, when this is the case, the bonds are almost collinear. In that case, it is a reasonable approximation to regard bonds ij and ik as *one* single bond and apply the torsion potential to bonds $(ij+ik \equiv jk)$, kl and jm , where sphere m is a neighbor of sphere j . If sphere j does not have any neighbors (except for sphere i), then $\Delta \mathbf{u}_{ij}$ would be zero anyway, and $\Delta \phi_{ijkl}$ would always be zero. The equation for

$\Delta \theta_{ijkl}$ is now obtained simply by replacing each index j by m and each index i by j , with $\mathbf{R}_{jk} \equiv \mathbf{R}_{ji} + \mathbf{R}_{ik}$. The case that bond kl is almost parallel to ik is treated in the same way.

The indeterminacy arising in the bond bending case for parallel \mathbf{R}_{ij} and \mathbf{R}_{kl} does not arise in the torsion potential, since \mathbf{R}_{ik} defines the plane into which the movement takes place. This does not hold if all three bonds are parallel, but that case can be circumvented in the way described previously.

It is important to note that the approach here presumes a more or less direct relationship between the spring network model and the microstructure of the porous material. Indeed, the elastic properties of the network, in terms of the spring constants k_{ij}^{CF} , k_{ijk}^{BB} , k_{ijkl}^T , are determined from the elastic properties of the matrix material, and from the geometry of the struts in the foam structure. This is distinctly different from most other approaches in the literature, where the spheres or nodes are usually arranged on a *regular* underlying lattice, e.g., square^{2,3} or triangular¹ in two dimensions, or simple or body-centered cubic (bcc),⁴⁻⁷ or hexagonal¹ in three dimensions. There, geometrical disorder is introduced by removing a number of bonds from the lattice according to some predefined probability distribution. The disordered network is considered to reflect a heterogeneous material, but without furnishing or assuming a relation with any actual material microstructure.

The model presented in this paper lends itself well for research on the effect of size effects on the fracturing process, and on the influence of pore size distribution. Van den Born *et al.*¹ and Arbabi and Sahimi⁴ were among the first to model compressive instead of tensile tests. This approach is also followed in this work. In the network representation of the porous microstructure, excluded volume effects have so far been neglected. Experimentally however, some compaction of top and bottom surfaces takes place at the beginning of the fracturing process. Spheres that got disconnected after bond failure may in certain configurations still transmit some load. The present network representation lends itself for inclusion of an additional potential term reflecting this.

Networks of the type considered here, with central force as well as bending and torsion interactions between nodes, can also be treated by other methods. In particular, such networks are completely similar to what are termed 'frameworks' in structural engineering. In that case, neighboring nodes are connected by a beam as a structural element. Bending and torsion are then incorporated by individual beams between two nodes, rather than by strings of three and four nodes, respectively, as in the present approach.³ This requires that each node not only has three displacements as degrees of freedom but also an orientation, measured by an additional three parameters (e.g., Euler angles). Thus, the geometric networks considered here can also be analyzed by computational structural mechanics techniques, especially the finite element method.^{12,13} The important difference with the present approach from a computational point of view, is that these finite element methods involve a more efficient method to incorporate bending and torsion, but the number of degrees of freedom in a given network is twice as large as in the present approach, where one has to solve three equations for each node.

The methodology has been tested for networks consisting

of up to 8000 nodes on a SGI Power Indigo,² a 75 MHz R8000 workstation with 256 Mbytes of RAM. In order to give an indication of the CPU time involved: the sample case presented in Figs. 5 and 6 (1000 spheres, 2701 bonds) needed 136 relaxation steps for complete failure (973 bonds broken) in 86 seconds CPU time for each relaxation step (stopping criterion for each relaxation step: $|\mathbf{K}\Delta\mathbf{u}-\Delta\mathbf{F}|/|\Delta\mathbf{F}|<\epsilon$, where $\epsilon=10^{-10}$). This depends very sensitively on the average number of bonds per node, because the four-body potential term is a third-nearest neighbor term. This number is strongly dependent on parameters in the configuration generation phase, such as the cut-off radius r_c (which is chosen to be as close to the bond percolation threshold as possible), and the parameters used in the Lennard-Jones potential. The sparse matrix solver used has not yet been optimized for computational speed however, since the main purpose of this work is to show that the pro-

posed methodology actually leads to global failure of the network. As mentioned before, a future paper will contain a more quantitative study of the network properties, notably the scaling properties of the ultimate strength as a function of the network size, the effect of the four-body term on CPU time, etc.

ACKNOWLEDGMENTS

The work described in this paper is part of the research program of the Foundation for Fundamental Research on Matter (FOM-Utrecht), has been supported by the Netherlands Organization for Scientific Research (NWO-The Hague) and IOP-METALS C94.703.RG.TF. The authors are grateful to Dr. Botta and Dr. Van der Ploeg for stimulating discussions and support on the numerical methods and to J. Kraak for assistance in the computer visualization part.

¹I. C. van den Born, A. Santen, H. D. Hoekstra, and J. Th. M. De Hosson, in *Fracture Processes in Concrete, Rock and Ceramics*, edited by J. J. M. van Mier, J. G. Rots, and A. Bakker (E & FN SPON, London, 1991), p. 231.

²S. Feng, P. N. Sen, B. I. Halperin, and C. J. Lobb, *Phys. Rev. B* **30**, 5386 (1984).

³H. J. Hermann, A. Hansen, and S. Roux, *Phys. Rev. B* **39**, 637 (1989).

⁴S. Arbabi and M. Sahimi, *Phys. Rev. B* **38**, 7173 (1988).

⁵M. Sahimi and S. Arbabi, *Phys. Rev. B* **47**, 695 (1993).

⁶J. Wang, *J. Phys. A* **22**, L291 (1989).

⁷S. Arbabi and M. Sahimi, *J. Phys. A* **23**, 2211 (1990).

⁸I. C. van den Born, A. Santen, H. D. Hoekstra, and J. Th. M. De Hosson, *Phys. Rev. B* **43**, 3794 (1991).

⁹M. P. Allen and D. J. Tildesley, *Computer Simulation of Liquids* (Oxford University Press, Oxford, 1992).

¹⁰S. P. Timoshenko, J. N. Goodier, *Theory of Elasticity*, 3rd ed. (McGraw-Hill, New York, 1982).

¹¹A. van der Ploeg, Ph.D. thesis, University of Groningen (1994).

¹²Y. Kantor and I. Webman, *Phys. Rev. Lett.* **52**, 1891 (1984).

¹³T. J. R. Hughes, *The Finite Element Method* (Prentice-Hall, Englewood Cliffs, NJ, 1987).